DOI: 10.1002/ejic.200800376

Beyond the Icosahedron: A Density Functional Theory Study of 14-Atom Germanium Clusters

R. Bruce King,*[a] Ioan Silaghi-Dumitrescu,[b] and Matei M. Uţă[b]

Keywords: Germanium / Metal clusters / Density functional theory

Density functional theory (DFT) at the hybrid B3LYP level has been applied to the germanium clusters Ge_{14}^{z} (z = –8, –6, –4, –2, 0, +2, +4) starting from seven different initial configurations. An O_h omnicapped cube structure is the most stable for Ge_{14}^{2-} followed by a hexagonal antiprism structure with a relative energy of 42.7 kcal/mol. The lowest-energy structure for neutral Ge_{14} is a triplet omnicapped cube with full O_h symmetry followed by a singlet omnicapped cube compressed to D_{4h} symmetry through Jahn–Teller distortion. The lowest energy Ge_{14}^{2+} structure is also an O_h structure derived from the omnicapped cube through elongation of the 12 edges of the underlying cube to give a rhomboidal dodecahedron with 12 rhombus faces. The lowest-energy Ge_{12}^{4+} structure is a bicapped icosahedron. Some D_{6h} hexagonal wheel structures at higher energies are also found for the hypoelectronic systems Ge_{14}, Ge_{14}^{2+}, and Ge_{14}^{4+}. The lowest-energy structures for the hyperelectronic Ge_{14}^{4-}, Ge_{14}^{6-}, and Ge_{14}^{8-} are relatively unsymmetrical not readily recognizable open structures typically with some pentagonal or hexagonal faces. The D_{6d} bicapped hexagonal antiprism found in 14-vertex C_2B_{12} carborane and $M_2C_2B_{10}$ dimetallacarborane structures is not the lowest-energy structure for any of the Ge_{14}^{z} clusters.

1. Introduction

In recent years the chemistry of supraicosahedral boranes has received considerable attention.[1,2] Such supraicosahedral boranes are based on polyhedra having more than the 12 vertices of the icosahedron. For the *closo*-boranes $B_nH_n^{2-}$ and isoelectronic carboranes with $2n + 2$ skeletal electrons the Wade–Mingos rules[3–6] suggest structures based on the most spherical deltahedra with all triangular faces and vertex degrees as nearly similar as possible. However, the smallest supraicosahedral boranes and particularly carboranes with 13 vertices do not always follow such rules. Thus, three different polyhedra are found in *closo*-carboranes $R_2C_2B_{11}H_{11}$ with the 28 skeletal electrons (= $2n + 2$ for $n = 13$) predicted by the Wade–Mingos rules and their metallacarborane analogues. In some cases the expected docosahedron with all triangular faces (22 of them)[7] is found, e.g. in several 13-vertex $(\eta^5\text{-}C_5H_5)CoC_2B_{10}H_{12}$ isomers. However, the docosahedron has two degree 6 vertices (starred in Figure 1), which are unfavorable structural features in polyhedral borane chemistry. Removal of one of the degree 6 vertices by breaking one of the edges from it leads to the henicosahedron with a single quadrilateral face (f_4) as well as 20 triangular faces. The henicosahedron is found in the metal-free carborane[8] 1,2-μ-$C_6H_4(CH_2)_2$-3-C_6H_5-1,2-$C_2B_{11}H_{10}$. The remaining degree 6 vertex in the henicosahedron can also be removed by breaking a second edge to give a ditrapezoidal icosahedron with two trapezoidal faces as well as 18 of the original triangular faces. Such a ditrapezoidal icosahedron is found[9] in 1,2-μ-$(CH_2)_3$-3-C_6H_5-1,2-$C_2B_{11}H_{10}$. None of these 13-vertex polyhedra has a particularly symmetrical structure.

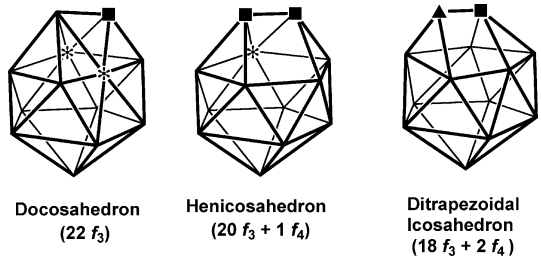

Figure 1. The three 13-vertex polyhedra found in the *closo*-carboranes $R_2C_2B_{11}H_{11}$ and their transition metal derivatives. Degree 6, 4, and 3 vertices in Figures 1 and 2 are indicated by stars, squares, and triangles, respectively.

The situation with 14-vertex polyhedra is considerably less complicated than that with the 13-vertex polyhedra, at least partially because of possibilities for more symmetrical structures. The 14-vertex deltahedron found in *closo*-borane and carborane derivatives with the 30 skeletal electrons (= $2n + 2$ for $n = 14$) predicted by the Wade–Mingos rules[3–6] is always the D_{6d} bicapped hexagonal antiprism with 12 de-

[a] Department of Chemistry, University of Georgia, Athens, Georgia 30602, USA
[b] Faculty of Chemistry and Chemical Engineering, Babeş-Bolyai University, Cluj-Napoca, Romania

Supporting information for this article is available on the WWW under http://www.eurjic.org or from the author.

gree 5 vertices at the vertices of two hexagonal "belts" and two degree 6 vertices on the C_6 axis (Figure 2). Examples of bicapped hexagonal antiprismatic boranes include the dimetallacarborane[7] (η^5-$C_5H_5)_2Co_2C_2B_{10}H_{12}$ and the metal-free carborane[10] (μ-$CH_2)_3C_2B_{12}H_{12}$.

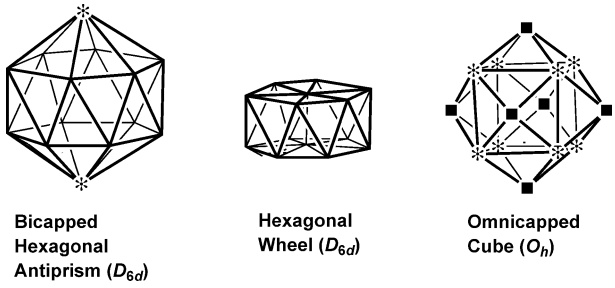

Figure 2. 14-Vertex deltahedra and related structures.

Bicapped hexagonal antiprismatic 14-vertex clusters do not appear to be found outside borane chemistry. However, moving the two axial (capping) vertices of the bicapped hexagonal antiprism towards the center and forming a bond between them inside the hexagonal prismatic cavity leads to a "hexagonal wheel" structure where the bond between the two axial vertices is the axle and the hexagons are the rims (Figure 2). An example of a hexagonal wheel structure is the cluster $[Al_{14}[N(SiMe_3)_2]_6I_6Li(OEt_2)_2]^-[Li(OEt_2)_4]^+$ reported by Schnöckel and co-workers.[11] A similar hexagonal wheel structure for the $Al_{14}I_{11}^-$ cluster observed experimentally by Castleman et al.[12,13] has been predicted by Han and Jung[14] using density functional theory.

Another highly symmetrical 14-vertex deltahedron is the omnicapped cube (Figure 2) with eight degree 6 vertices and six degree 4 vertices and O_h symmetry. A relatively early example of a 14-vertex omnicapped cube cluster is the carbonylnickel complex (μ_4-$C_6H_5P)_6Ni_8(CO)_8$, in which the phosphorus vertices cap the faces of an underlying Ni_8 cube.[15] The omnicapped cube is also found in a variety of 14-vertex aluminum clusters with various skeletal electron counts[16] including carbalane clusters of the general formula $(AlX)_8(\mu_4\text{-}CR)_6^{2-}$ with 36 skeletal electrons with the carbon atoms capping the faces of an Al_8 cube[17,18] as well as the silicon-centered cluster[19] $Al_8(\mu_8\text{-}Si)(\mu_4\text{-}AlCp^*)_6$ with 24 skeletal electrons according to the Wade–Mingos[3–6] electron-counting rules. However, if the otherwise external lone pairs of the underlying Al_8 cube in $Al_8(\mu_8\text{-}Si)(\mu_4\text{-}AlCp^*)_6$ are also counted, then the omnicapped cube in this cluster becomes a 24 + (8)(2) = 40-electron system, which is a favored number using the jellium model.[20,21]

The research discussed in this paper extends our DFT studies to clusters with more than 12 vertices in order to study effects of electron count on supraicosahedral cluster geometry. The 14-vertex systems were chosen in preference to the 13-vertex systems because of their higher symmetry and greater variety outside polyhedral borane and carborane chemistry. The germanium clusters Ge_{14}^z (z = –8, –6, –4, –2, 0, +2, +4) without interstitial atoms were chosen as tractable systems having vertices isolobal to either the BH vertices in borane structures or the AlX and CR vertices in carbalane structures. In addition, the study of germanium clusters provide reasonable models for clusters of other group 14 elements except carbon, particularly silicon and tin. The range of charges on Ge_{14}^z chosen for this work spans the 36 skeletal electrons found in the carbalane clusters $(AlX)_8(\mu_4\text{-}CR)_6^{2-}$ to the 24 skeletal electrons found in the silicon-centered cluster $Al_8(\mu_8\text{-}Si)(\mu_4\text{-}AlCp^*)_6$ and the carbonylmetal derivative $(\mu_4\text{-}C_6H_5P)_6Ni_8(CO)_8$. Isoelectronic and isolobal relationships provide analogies of our DFT results on Ge_{14}^z clusters to experimentally known structures. The DFT methods used in this work are well established having previously been used by our group to study bare germanium clusters having five to twelve germanium atoms.[22–27]

2. Theoretical Methods

Computations were carried out at the hybrid DFT B3LYP level[28–31] with the 6-31G(d) (valence) double zeta quality basis functions extended by adding one set of polarization (d) functions. The Gaussian 98 package of programs[32] was used in which the fine grid (75, 302) is the default for numerically evaluating the integrals, and the tight (10^{-8}) hartree stands as default for the self-consistent field convergence. Optimizations were carried out starting with seven structures including examples of 14-vertex polyhedra exhibiting octahedral, sevenfold and sixfold symmetry, as well as two structures of D_{3d} and D_{4h} symmetry derived from the omnicapped octahedron (Figure 3).

The symmetries were maintained during the geometry optimization processes. In addition, symmetry breaking using modes defined by imaginary vibrational frequencies was used to determine optimized structures with minimum energies. Vibrational analyses show that all of the final optimized structures discussed in this paper are genuine minima at the B3LYP/6-31G(d) level without any significant imaginary frequencies. In a few cases, particularly for some of the hypoelectronic structures, the calculations ended with acceptable small imaginary frequencies,[33] and these values are indicated in the corresponding figures.

The optimized structures found for the Ge_{14}^z clusters are labeled by the number of skeletal electrons and relative energies. Thus, the lowest-energy structure with 30 skeletal electrons (i.e., Ge_{14}^{2-}) is designated as **30-1**. Triplet structures are indicated by a **T** after the structure label. More details of all of the optimized structures, including all interatomic distances and the initial geometries leading to a given optimized structure, are provided in the Supporting Information. In assigning polyhedra to the optimized structures, the Ge–Ge distances less than 3.2 Å were normally considered as polyhedral edges.

In most cases only structures within 20 kcal/mol of the global minima are discussed in this paper. More comprehensive information including the higher energy structures is presented in the Supporting Information.

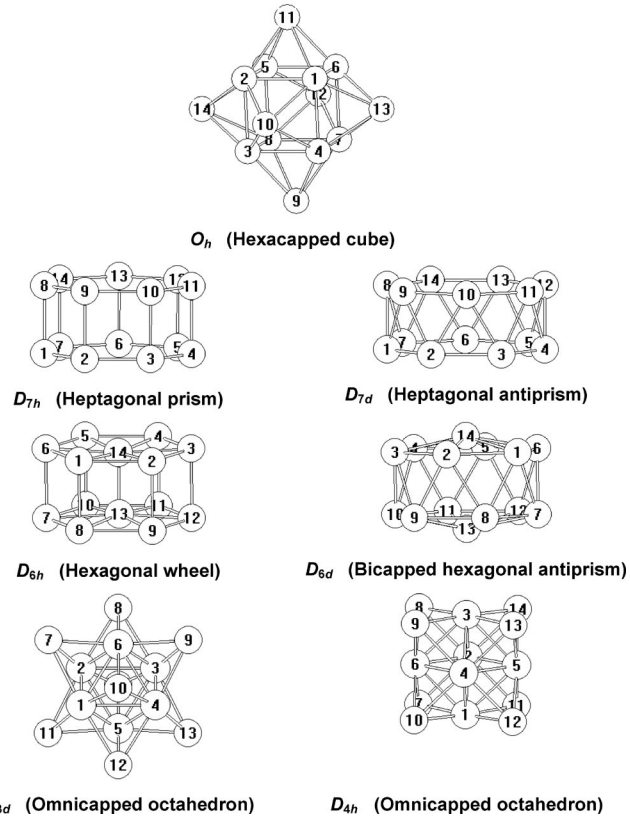

Figure 3. The seven initial 14-vertex polyhedra used as starting points.

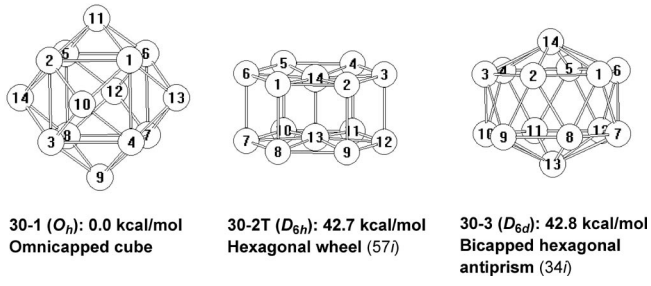

Figure 4. The lowest-energy structures found for Ge_{14}^{2-}.

3. Results and Discussion

3.1 The 30 Skeletal Electron Ge_{14}^{2-}

The 30 skeletal electron Ge_{14}^{2-} is the $2n + 2$ skeletal electron system for a 14-atom cluster and thus is expected by the Wade–Mingos rules[3–6] to have a deltahedral structure. The lowest-energy structure **30-1** found for Ge_{14}^{2-} (Figure 4) is indeed a deltahedron, but the O_h omnicapped cube rather than the D_{6d} bicapped hexagonal prism found for the isoelectronic boranes[7,10] such as $(\eta^5\text{-}C_5H_5)_2Co_2C_2B_{10}H_{12}$ and $(\mu\text{-}CH_2)_3C_2B_{12}H_{12}$. The two unique Ge–Ge edge lengths in structure **30-1** are 2.963 Å for the underlying cube edges and 2.537 Å from a capping vertex to an underlying cube vertex.

The D_{6h} triplet hexagonal wheel **30-2T** (Figure 4) is also found for Ge_{14}^{2-}, but at a very high relative energy of 42.7 kcal/mol above the lowest-energy structure **30-1**. A D_{6d} bicapped hexagonal antiprism structure **30-3** is also found for Ge_{14}^{2-} at essentially the same energy as the triplet hexagonal wheel.

3.2 Hyperelectronic Structures

None of the structures found within 30 kcal/mol of the lowest-energy structure **32-1** of Ge_{14}^{4-} (Figure 5) are recognizable as *nido* polyhedra having all triangular faces except for a single non-triangular face in accord with expectations from the Wade–Mingos rules.[3–6] The lowest-energy structure **32-1** for Ge_{14}^{4-} is an unusual polyhedron with six pentagonal faces and three pairs of triangular faces with each pair sharing an edge. The symmetry point group looks like D_{3h}, but actually this symmetry is broken upon optimization. Thus, the three edges Ge7–Ge8, Ge9–Ge13, and Ge11–Ge12, which would be equivalent under D_{3h} symmetry, instead are 2.68 Å, 2.64 Å, and 2.68 Å, respectively, in **32-1**. Furthermore, the three edges Ge1–Ge2, Ge4–Ge5, and Ge6–Ge3 (equivalent under D_{3h} symmetry) are 2.84 Å, 2.76 Å, and 2.76 Å, respectively, in **32-1**.

The other two structures for Ge_{14}^{4-} within ca. 10 kcal/mol of **32-1** are completely unsymmetrical and not obviously recognizable. Structure **32-3** at 10.1 kcal/mol above **32-1** is a highly flattened (oblate) structure.

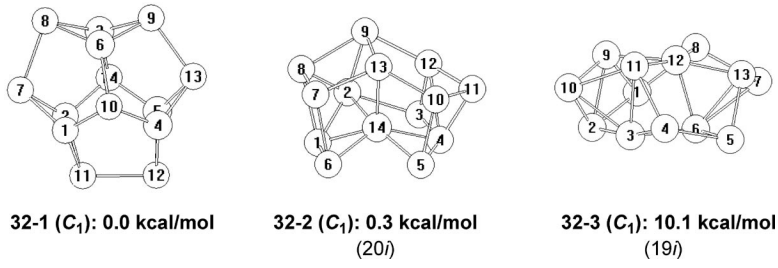

Figure 5. The lowest-energy structures found for Ge_{14}^{4-}.

The lowest-energy structure for Ge_{14}^{6-}, namely **34-1** (Figure 6) is an open non-polyhedral structure with four degree 3 vertices and three hexagonal faces. No other Ge_{14}^{6-} structure was found within 38 kcal/mol of this rather unusual structure.

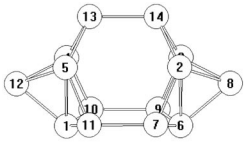

Figure 6. The lowest-energy structure found for Ge_{14}^{6-}. No other Ge_{14}^{6-} structure was found within 38 kcal/mol of this lowest-energy structure.

Three structures were found for Ge_{14}^{8-} within 50 kcal/mol of the lowest-energy structure **36-1** (Figure 7). The two lowest-lying structures **36-1** and **36-2** are not obviously recognizable and are very different from the omnicapped cube structures found for carbalanes of the type $(AlX)_8(\mu_4\text{-}CR)_6^{2-}$ with 36 apparent skeletal electrons. A triplet heptagonal prismatic structure **36-3T** is found for Ge_{14}^{8-} at 20.4 kcal/mol above the lowest-energy structure **36-1**.

3.3 The Neutral Ge_{14}

The neutral Ge_{14} cluster is certainly unstable with respect to polymerization to bulk germanium metal. However, computations on neutral Ge_{14} are of interest in order to characterize the relative stabilities of various 14-vertex polyhedra in 28 skeletal electron systems.

The lowest-energy structure **28-1T** for Ge_{14} is a triplet omnicapped cube within 0.01 Å of having ideal O_h symmetry (Figure 8). The lowest-lying singlet structure for neutral Ge_{14}, namely **28-2** (Figure 8), is also based on an omnicapped cube, but compressed so that the ideal O_h symmetry is reduced to D_{4h} symmetry. The final structure for Ge_{14} within 25 kcal/mol of the lowest-energy structure **28-1** is the singlet D_{6h} hexagonal wheel structure **28-3** (Figure 8) at 10.0 kcal/mol above **28-1**.

3.4 Other Hypoelectronic Structures

The highly symmetrical (O_h) lowest-energy structure **26-1** for Ge_{14}^{2+} (Figure 9) is a rhomboidal dodecahedron with 12 equivalent rhombus faces and 24 equivalent edges of length 2.562 Å. Six of the vertices have degree 4 vertices, whereas the remaining eight vertices have degree 3. The other structure for Ge_{14}^{2+} within 25 kcal/mol above the lowest-energy structure **26-1** is the triplet hexagonal wheel **26-2T** at 17.0 kcal/mol above **26-1**.

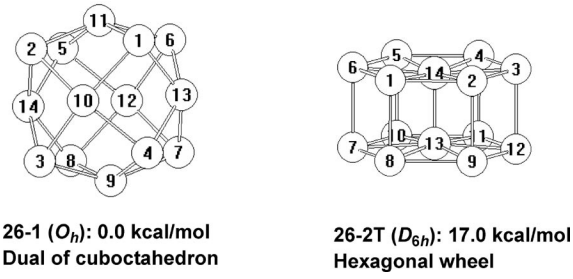

Figure 9. The lowest-energy structures for Ge_{14}^{2+}.

The lowest energy structure **24-1** for Ge_{14}^{4+} (Figure 10) is a bicapped icosahedron. Three other Ge_{14}^{4+} structures are found within 20 kcal/mol of this lowest-energy structure. The next higher lying Ge_{14}^{4+} structure **24-2** is a highly unsymmetrical (clearly C_1) rather flat (oblate) structure at

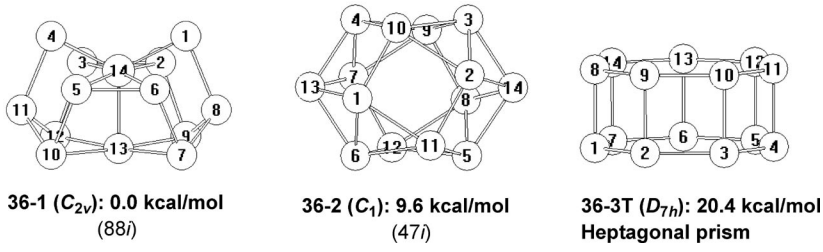

Figure 7. The lowest-energy structures found for Ge_{14}^{8-}.

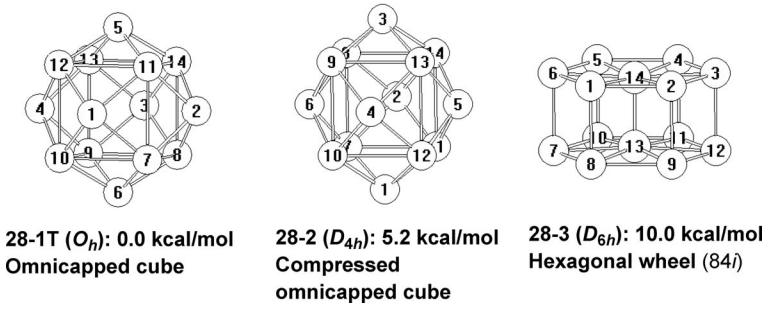

Figure 8. The lowest-energy structures found for Ge_{14}.

5.2 kcal/mol above **24-1**. In addition, two hexagonal wheel structures are found for Ge_{14}^{4+} at energies of 11.9 kcal/mol for **24-3** and 13.7 kcal/mol for **24-4** (Figure 10).

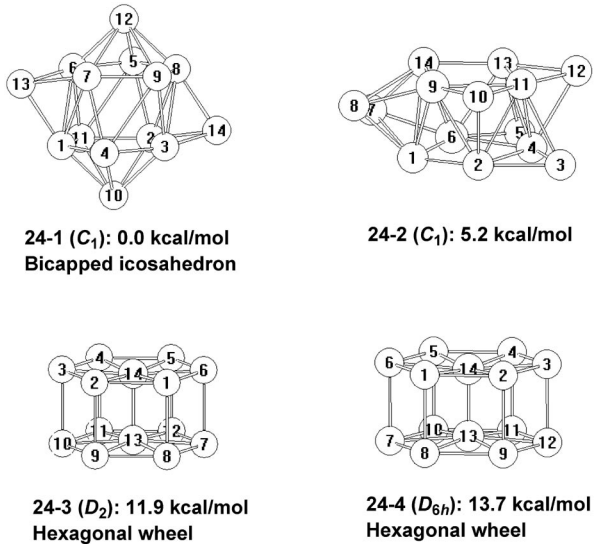

Figure 10. The lowest-energy structures for Ge_{14}^{4+}.

4. Discussion

4.1 Geometries

The two geometries found for Ge_{14}^{z} with several different skeletal electron counts are the omnicapped cube and the hexagonal wheel (Figure 11). The variations in their detailed geometries as a function of skeletal electron count have been examined as discussed below. The D_{6d} bicapped hexagonal antiprism found in 14-vertex borane derivatives[10] such as $(\mu\text{-}CH_2)_3C_2B_{12}H_{12}$ is found only in Ge_{14}^{2-} and then only at a very high energy (42.7 kcal/mol) relative to the omnicapped cube lowest-energy structure (Figure 4).

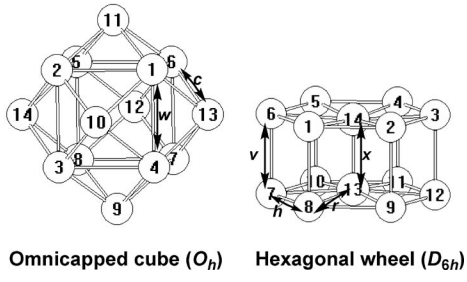

Figure 11. The different types of edges in the omnicapped cube and the hexagonal wheel.

4.1.1 The O_h Omnicapped Cube

This deltahedral geometry with only degree 4 and 6 vertices and ideal O_h symmetry is the lowest-energy structure for singlet Ge_{14}^{2-} (**30-1**) and triplet Ge_{14} (**28-1T**). In addition, a compressed omnicapped cube with D_{4h} symmetry is found in singlet Ge_{14} (**28-2**). This distortion arises from the Jahn–Teller effect. The O_h rhomboid dodecahedron (cuboctahedron dual) found to be the lowest-energy structure **26-1** for Ge_{14}^{2+} can be derived from the omnicapped cube by lengthening the edges of the underlying cube beyond the maximum bonding distance, considered here to be 3.2 Å.

Table 1 summarizes the geometrical features of the omnicapped cube and related structures for the Ge_{14}^{z} clusters in terms of the two independent edge lengths, namely the edge lengths, *w*, of the underlying cube and the lengths, *c*, of the edges to the capping vertices (Figure 11). Removal of electron pairs from Ge_{14}^{2-} to give first Ge_{14} and then Ge_{14}^{2+} is seen to increase significantly the edge lengths of the underlying cube while having very little effect on the lengths of the edges to the capping vertices. When Ge_{14}^{2+} is reached, the "edge length" of the underlying cube becomes 3.451 Å, which is considered too long to be an actual edge. The omnicapped cube in **26-1** thus has effectively undergone a dodecuple (12-fold) "diamond-square" process[34] (actually a "diamond-rhombus" process) retaining the O_h symmetry. The resulting new polyhedron has 12 equivalent rhombus faces and is the dual of the cuboctahedron.

Table 1. Dimensions of the structures derived from the omnicapped cube for Ge_{14}^{z} ($z = -2, 0, +2$). The numbers of equivalent distances are given in parentheses.

Structure	Symmetry	Cube edge, *w* [Å]	Capping edge, *c* [Å]
Ge_{14}^{2-} (**30-1**)	O_h	2.983 (12)	2.537 (24)
Ge_{14} (**28-1T**)	O_h	3.112 (6), 3.117 (6)	2.509 (24)
Ge_{14} (**28-2**)	D_{4h}	3.025 (4), 3.155 (8)	2.540 (16), 2.455 (8)
Ge_{14}^{2+} (**26-1**)	O_h	3.451 (12)	2.526 (24)

The structures of the different Ge_{14}^{z} clusters with geometries derived from the omnicapped cube can be related to their frontier molecular orbitals (Figure 12). In the omnicapped cube lowest-energy structure of Ge_{14}^{2-} (**30-1** in Figure 4) the HOMO is a fully occupied pair of degenerate e_g orbitals. There are two possibilities for a two-electron oxidation of Ge_{14}^{2-} (**30-1**) to neutral Ge_{14}. Removal of one electron from each component of the e_g HOMO of **30-1** gives the triplet **28-1T** (Figure 8), which is the lowest-energy structure of Ge_{14}. The O_h symmetry of **30-1** is retained in this process. The second alternative is to remove two electrons from one of the components of the e_g HOMO of **30-1** to give singlet Ge_{14}. This, however, lifts the degeneracy of the e_g HOMO leading to a filled a_g HOMO and an empty b_g LUMO resulting in a Jahn–Teller distortion, thereby reducing the symmetry from O_h to D_{4h}. The existence of both O_h triplet Ge_{14} and D_{4h} singlet Ge_{14} structures (at least in silico) with the topology of the original omnicapped cube is analogous to cyclobutadiene being either a square D_{4h} triplet or a rectangular D_{2h} singlet.[35,36]

The doubly degenerate HOMO of Ge_{14}^{2-} (**30-1**) is seen to be bonding in the underlying cube (Figure 12). Removal of all four electrons from this HOMO to convert Ge_{14}^{2-} to Ge_{14}^{2+} is therefore expected to increase significantly the edge lengths of the underlying cube (*w* in Table 1) while retaining the original O_h symmetry of the omnicapped cube. This is consistent with the lowest-energy structure **26-1** (Figure 9) in which the original edges of the underlying

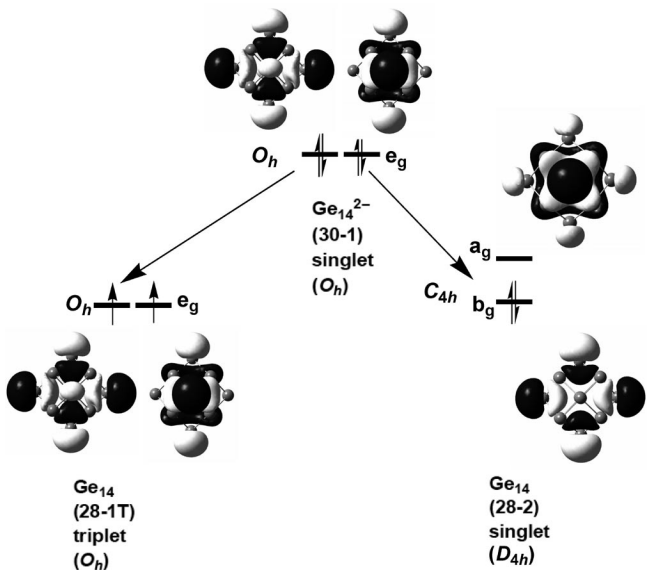

Figure 12. The effect on the doubly degenerate e_g HOMO upon two-electron oxidation of Ge_{14}^{2-} (**30-1** in Figure 4) to Ge_{14}.

cube in Ge_{14}^{2-} have been lengthened to a "non-bonding" distance of 3.451 Å while retaining the O_h symmetry. Thus, the polyhedron of Ge_{14}^{2+} (**26-1**) is best described as a rhomboidal dodecahedron with 12 rhombus faces. Note that the global minima for Ge_{14}^{2-}, Ge_{14}, and Ge_{14}^{2+} are all derived from the omnicapped cube.

4.1.2 The D_{6h} Hexagonal Wheel

The D_{6h} hexagonal wheel structure is found for energetically competitive structures for Ge_{14}^{2-}, Ge_{14}, Ge_{14}^{2+}, and Ge_{14}^{4+}, although never as a lowest-energy structure. The geometrical details of these hexagonal wheel structures in terms of the lengths of the four distinct types of edges (Figure 11) are given in Table 2, and their frontier orbitals are depicted in Figure 13.

The HOMO for the most highly reduced member of this series of hexagonal wheel structures, namely Ge_{14}^{2-} (**30-2T**), is a pair of half-filled doubly degenerate e_{2u} orbitals consistent with its triplet spin multiplicity (Figure 13). Two-electron oxidation of **30-2T** to the hexagonal wheel neutral Ge_{14} (**28-3**) empties these e_{2u} orbitals, which are antibonding along the vertical edges of the cluster (*v* in Figure 11). This is consistent with the predicted shortening of the vertical distances from 2.589 Å in **30-2T** to 2.532 Å in **28-3** (Table 2).

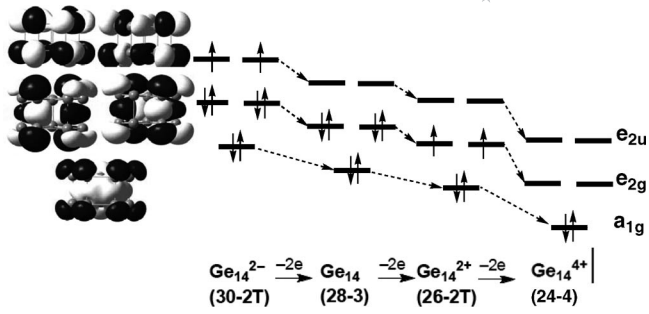

Figure 13. The frontier molecular orbitals for the series of hexagonal wheels Ge_{14}^{z} ($z = -2 \rightarrow 0 \rightarrow +2 \rightarrow +4$).

The HOMO in Ge_{14} (**28-3**) is a doubly degenerate pair of e_{2g} orbitals, which are bonding along the vertical edges of the cluster (Figure 13). Further two-electron oxidation of **28-3** to Ge_{14}^{2+} removes half of the electrons from this pair of e_{2g} orbitals (Figure 13) leading to a triplet hexagonal wheel Ge_{14}^{2+} structure, still with the full D_{6h} symmetry. The vertical edges of the hexagonal wheel (*v* in Figure 11) now lengthen from 2.532 Å in **28-3** to 2.580 Å in **26-2T**. An additional two-electron oxidation of the triplet hexagonal wheel Ge_{14}^{2+} (**26-2T**) to give the singlet hexagonal wheel Ge_{14}^{4+} (**24-4**) completely empties the pair of degenerate e_{2g} orbitals. This leads to a further increase in the vertical edge lengths of the hexagonal wheel from 2.580 Å to 2.623 Å (Table 2).

4.2 Comparison of Analogous Ge_n^{2-} and $B_nH_n^{2-}$ Clusters

The Ge_{14}^{2-} system is interesting because its lowest-energy structure, namely the O_h omnicapped cube **30-1** (Figure 4), is different from the D_{6d} bicapped hexagonal antiprism (Figure 2) found experimentally in isoelectronic carborane derivatives of the general type $R_2C_2B_{12}H_{12}$, among which $(\mu\text{-}CH_2)_3C_2B_{12}H_{12}$ has been synthesized and structurally characterized by X-ray diffraction.[10] The $Ge_{14}^{2-}/B_{14}H_{14}^{2-}$ system ($n = 14$) is the third example of a $Ge_n^{2-}/B_nH_n^{2-}$ system where the lowest-energy structure for a Ge_n^{2-} cluster is different from that of the corresponding $B_nH_n^{2-}$ cluster. The other examples are the eight-vertex[24] ($n = 8$) and eleven-vertex[25] ($n = 11$) systems (Figure 14). In all three cases the lowest-energy polyhedra for both the Ge_n^{2-} and $B_nH_n^{2-}$ systems are deltahedra, i.e. polyhedra with all triangular faces, in accord with expectations from the Wade–Mingos rules.[3–6] However, the lowest-energy deltahedral structures for $B_nH_n^{2-}$ ($n = 8, 11, 14$) contain the maximum number of

Table 2. Dimensions of the structures derived from the hexagonal wheel for Ge_{14}^{z} ($z = -2, 0, +2, +4$). The numbers of equivalent distances are given in parentheses.

Structure	Symmetry	*v* [Å]	*h* [Å]	*r* [Å]	*x* [Å]
Ge_{14}^{2-} (**30-2T**)	D_{6h}	2.589 (6)	2.613 (12)	2.618 (12)	2.261 (1)
Ge_{14} (**28-3**)	D_{6h}	2.532 (6)	2.593 (12)	2.597 (12)	2.250 (1)
Ge_{14}^{2+} (**26-2T**)	D_{6h}	2.580 (6)	2.597 (12)	2.602 (12)	2.257 (1)
Ge_{14}^{4+} (**24-3T**)	D_2	2.540 (4), 2.676 (4), 2.677 (4)	2.633 (4), 2.647 (2)	2.697 (8), 2.506 (4)	2.372 (1)
Ge_{14}^{4+} (**24-4**)	D_{6h}	2.623 (12)	2.657 (6)	2.630 (12)	2.272 (1)

degree 5 vertices in accord with the previously recognized special stability of degree 5 boron vertices.[37–40] By contrast, none of the lowest-energy structures of the corresponding Ge_n^{2-} clusters (n = 8, 11, 14) contain any degree 5 vertices. This suggests that degree 5 vertices are much less favorable for germanium clusters than for borane clusters.

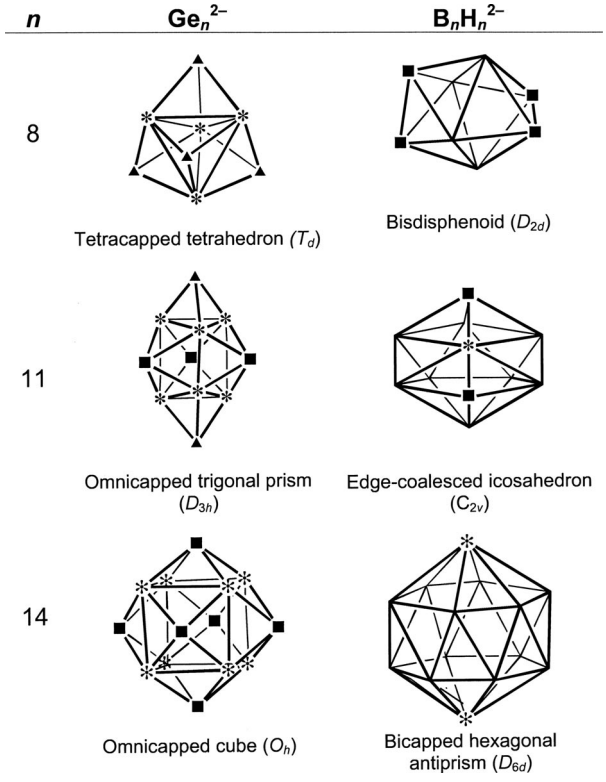

Figure 14. The lowest-energy Ge_n^{2-} and $B_nH_n^{2-}$ structures for n = 8, 11, 14. Degree 6, 4, and 3 vertices are indicated by stars, squares, and triangles, respectively.

Among the 8-, 11-, and 14-vertex $Ge_n^{2-}/B_nH_n^{2-}$ systems (Figure 14), the 14-vertex system is particularly interesting, because the Ge_{14}^{2-} O_h omnicapped cube lies a very large 42.7 kcal/mol below the Ge_{14}^{2-} D_{6d} bicapped hexagonal antiprism found to be the favored polyhedron for 14-vertex carboranes of the type $R_2C_2B_{12}H_{12}$ [e.g., R_2 = $-(CH_2)_3-$].[10] By comparison, for the 11-vertex system the approximately D_{3h} lowest-energy structure for Ge_{11}^{2-} lies only 5.2 kcal/mol below the C_{2v} edge-coalesced icosahedron found in the chemistry of 11-vertex boranes such as $B_{11}H_{11}^{2-}$, $C_2B_9H_9$, and their substitution products. Similarly, for the 8-vertex system the T_d tetracapped tetrahedron lowest-energy structure for Ge_8^{2-} lies only 3.9 kcal/mol below the D_{2d} bis(disphenoid) found in the chemistry of 8-vertex boranes.

5. Summary

Simple application of the Wade–Mingos rules[3–6] suggests a bicapped hexagonal antiprism for Ge_{14}^{2-} similar to that found experimentally in the isoelectronic carborane $(\mu\text{-}CH_2)_3C_2B_{12}H_{12}$ and related dimetallacarboranes. However, our DFT studies predict the more symmetrical O_h omnicapped cube to lie approximately 43 kcal/mol below the bicapped hexagonal antiprism for Ge_{14}^{2-}. The global minima for the hypoelectronic Ge_{14} and Ge_{14}^{2+} are also derived from the omnicapped cube. Hexagonal wheel D_{6h} structures are also found for Ge_{14}, Ge_{14}^{2+}, and Ge_{14}^{4+} at competitive energies. The lowest-energy structures for the hyperelectronic Ge_{14}^{4-}, Ge_{14}^{6-}, and Ge_{14}^{8-} are relatively unsymmetrical not readily recognizable open structures, typically with some pentagonal or hexagonal faces.

Supporting Information (see footnote on the first page of this article): Optimized Ge_{14}^{z} structures and geometries listed according to the starting structures.

Acknowledgments

We are indebted to the National Science Foundation for partial support of this work under Grants CHE-0209857 and CHE-0716718. Part of this work was undertaken with the financial support from CEEX-42 SUPRAMOL program, Romania.

[1] R. B. King, *J. Organomet. Chem.* **2007**, *692*, 1773.
[2] L. Deng, Z. W. Xie, *Coord. Chem. Rev.* **2007**, *251*, 2452.
[3] K. Wade, *J. Chem. Soc., Chem. Commun.* **1971**, 792.
[4] K. Wade, *Adv. Inorg. Chem. Radiochem.* **1976**, *18*, 1.
[5] D. M. P. Mingos, *Nature Phys. Sci.* **1972**, *99*, 236.
[6] D. M. P. Mingos, *Accts. Chem. Res.* **1984**, *17*, 311.
[7] D. F. Dustin, G. B. Dunks, M. F. Hawthorne, *J. Am. Chem. Soc.* **1973**, *95*, 1109.
[8] A. Burke, D. Ellis, B. T. Giles, B. E. Hodson, S. A. Macgregor, G. M. Rosair, A. J. Welch, *Angew. Chem. Int. Ed.* **2003**, *42*, 225.
[9] L. Deng, H. S. Chen, Z. Xie, *J. Am. Chem. Soc.* **2006**, *128*, 5219.
[10] L. Deng, H. S. Chen, Z. Xie, *Angew. Chem. Int. Ed.* **2005**, *44*, 2128.
[11] H. Köhnlein, G. Stösser, E. Baum, E. Möllhausen, U. Huniar, H. Schnöckel, *Angew. Chem. Int. Ed.* **2000**, *39*, 799.
[12] D. E. Bergeron, P. J. Rosch, W. Castleman Jr, N. O. Jones, S. N. Khanna, *Science* **2005**, *307*, 231.
[13] H. O. Jones, J. U. Reveles, S. N. Khanna, D. E. Bergeron, P. J. Rosch, A. W. Castleman, *J. Chem. Phys.* **2006**, *124*, 154311.
[14] Y.-K. Han, J. Jung, *J. Chem. Phys.* **2006**, *125*, 084101.
[15] L. D. Lower, L. F. Dahl, *J. Am. Chem. Soc.* **1976**, *98*, 5046.
[16] B. Creton, S. Kahlal, M. T. Garland, Z. Lin, J.-F. Halet, J.-Y. Saillard, *J. Cluster Sci.* **2007**, *18*, 271.
[17] A. Stasch, H. W. Vicovic, D. Roesky, J. Magull, H.-G. Schmidt, M. Noltemeyer, *Inorg. Chem.* **2004**, *43*, 3625.
[18] A. Stasch, H. W. Roesky, M. Noltemeyer, H.-G. Schmidt, *Inorg. Chem.* **2005**, *44*, 5854.
[19] A. Purath, C. Dohmeier, A. Ecker, R. Köppe, H. Krautscheid, H. Schnöckel, R. Alrich, C. Stoermer, J. Friedrich, P. Jutzi, *J. Am. Chem. Soc.* **2000**, *122*, 6955.
[20] W. A. De Heer, *Rev. Mod. Phys.* **1993**, *65*, 611.
[21] R. B. King, I.Silaghi-Dumitrescu, *Dalton Trans.*, in press.
[22] R. B. King, I. Silaghi-Dumitrescu, A. Kun, *J. Chem. Soc., Dalton Trans.* **2002**, 3999.
[23] R. B. King, I. Silaghi-Dumitrescu, *Inorg. Chem.* **2003**, *42*, 6701.
[24] R. B. King, I. Silaghi-Dumitrescu, A. Lupan, *Inorg. Chem.* **2005**, *44*, 3579.
[25] R. B. King, I. Silaghi-Dumitrescu, A. Lupan, *Dalton Trans.* **2005**, 1858.
[26] R. B. King, I. Silaghi-Dumitrescu, M. M. Uţă, *Inorg. Chem.* **2006**, *45*, 4974.
[27] R. B. King, I. Silaghi-Dumitrescu, M. M. Uţă, *Dalton Trans.* **2007**, 364.
[28] S. H. Vosko, L. Wilk, M. Nusair, *Can. J. Phys.* **1980**, *58*, 1200.

[29] A. D. Becke, *J. Chem. Phys.* **1993**, *98*, 5648.
[30] P. J. Stephens, F. J. Devlin, C. F. Chabalowski, M. J. Frisch, *J. Phys. Chem.* **1994**, *98*, 11623.
[31] C. Lee, W. Yang, R. G. Parr, *Phys. Rev. B* **1998**, *37*, 785.
[32] M. J. Frisch, G. W. Trucks, H. B. Schlegel, G. E. Scuseria, M. A. Robb, J. R. Cheeseman, V. G. Zakrzewski, J. A. Montgomery Jr, R. E. Stratmann, J. C. Burant, S. Dapprich, J. M. Millam, A. D. Daniels, K. N. Kudin, M. C. Strain, O. Farkas, J. Tomasi, V. Barone, M. Cossi, R. Cammi, B. Mennucci, C. Pomelli, C. Adamo, S. Clifford, J. Ochterski, G. A. Petersson, P. Y. Ayala, Q. Cui, K. Morokuma, N. Rega, P. Salvador, J. J. Dannenberg, D. K. Malick, A. D. Rabuck, K. Raghavachari, J. B. Foresman, J. Cioslowski, J. V. Ortiz, A. G. Baboul, B. B. Stefanov, G. Liu, A. Liashenko, P. Piskorz, I. Komaromi, R. Gomperts, R. L. Martin, D. J. Fox, T. Keith, M. A. Al-Laham, C. Y. Peng, A. Nanayakkara, M. Challacombe, P. M. W. Gill, B. Johnson, W. Chen, M. W. Wong, J. L. Andres, C. Gonzalez, M. Head-Gordon, E. S. Replogle, J. A. Pople, *Gaussian 98*, Revision A.11.3, Gaussian, Inc., Pittsburgh PA, **2002**..
[33] Y. Xie, H. F. Schaefer III, R. B. King, *J. Am. Chem. Soc.* **2000**, *122*, 8746.
[34] W. N. Lipscomb, *Science* **1966**, *153*, 373.
[35] V. I. Minkin, M. N. Glukhovtsev, B. Ya. Simkin, *Aromaticity and Antiaromaticity: Electronic and Structural Aspects*, Wiley-Interscience, New York, **1994**.
[36] K. B. Wiberg, *Chem. Rev.* **2001**, *101*, 1317.
[37] R. E. Williams, *Chem. Rev.* **1992**, *92*, 177.
[38] E. D. Jemmis, P. N. V. Pavankumar, *Proc. Indian Acad. Sci. Chem. Sci.* **1984**, *93*, 479.
[39] I. Boustani, *J. Solid State Chem.* **1997**, *133*, 182.
[40] R. B. King, *Inorg. Chem.* **2001**, *40*, 6369.

Received: April 14, 2008
Published Online: July 30, 2008

